Kidney International, Vol. 45 (1994), pp. 1369–1380

Coupling of cell volume and membrane potential changes to fluid secretion in a model of renal cysts

LAWRENCE P. SULLIVAN, DARREN P. WALLACE, and JARED J. GRANTHAM

Department of Physiology and Nephrology Division, Department of Medicine, University of Kansas Medical Center, Kansas City, Kansas, USA

Coupling of cell volume and membrane potential changes to fluid secretion in a model of renal cysts. Renal tubular epithelia ordinarily absorb NaCl and water, although recent evidence indicates that renal cysts secrete fluid. We have utilized the experimental advantages offered by cultured cysts, formed in a collagen matrix by propagating Madin-Darby canine kidney cells, to investigate the mechanisms involved in fluid secretion by this renal epithelium. The rate of fluid transport (adduced from changes in cavity volume), cell volume and changes in membrane potential were measured simultaneously in isolated cysts. Under basal conditions, cysts absorbed fluid ($-0.83 \pm 0.34 \times 10^{-6}$ ml/min/cm^2 cavity surface area, $N = 23$). AVP and IBMX changed the direction of net fluid transport to secretion ($4.24 \pm 0.49 \times 10^{-6}$ ml/min/cm^2). Cell volume initially fell 7.4 ± 0.5% and remained stable thereafter as secretion continued. Membrane electrical potential (bis-oxonol epifluorescence) hyperpolarized in 13 cysts and depolarized in 6, the mean change was 1.9 ± 3.1%. Fluid secretion was abolished by 0.1 mM ouabain. Secretion was not affected by 0.1 mM DIDS and cell pH (bis-carboxyethyl-carboxyfluorescein epifluorescence) was not altered by the induction of secretion, suggesting that secretion is not dependent on Cl-HCO_3 exchange. Barium, in the presence of AVP and IBMX, depolarized the cell membrane potential (bis-oxonol fluorescence increased 22.3 ± 0.03%), reversed secretion to absorption (from 3.21 ± 0.93 to $-1.52 \pm 0.61 \times 10^{-6}$ ml/min/cm^2), and increased cell volume 2.7 ± 0.5%. Bumetanide (100 μM) reduced fluid secretion from 4.49 ± 1.23 to $-0.75 \pm 0.55 \times 10^{-6}$ ml/min/cm^2, further reduced cell volume 4.4 ± 1.2% and hyperpolarized the membranes (bis-oxonol fluorescence fell 24.3 ± 5.0%). In the absence of AVP and IBMX bumetanide had no effect on fluid transport, cell volume or membrane potentials. We conclude that AVP reversed the direction of fluid transport in these cultured renal epithelial cysts from absorption to secretion by stimulating a coordinated interaction of basolateral and apical K, Cl and Na transport mechanisms.

Vectorial fluid transport is an important function of polarized epithelia. Nearly all renal tubular segments absorb fluid as a secondary consequence of the net absorption of osmotic solute [1]. Although the ability to reverse the direction of net fluid transport to secretion is typical of other absorptive epithelia, for instance the intestine, the capacity of the renal epithelia to secrete fluid has not been widely recognized [2]. The recent direct demonstration that cystic epithelia removed from patients with autosomal-dominant polycystic kidney disease secrete fluid in response to adenylate cyclase agonists [3] accentuates our lack of knowledge regarding the solute transport systems involved in secretion by renal epithelia and the factors that regulate that transport. In an effort to obtain such knowledge, we have adapted techniques to study *in vitro* the processes involved in fluid secretion by cultured renal epithelia. We have applied these techniques initially to a strain of renal epithelial cells, Madin-Darby canine kidney cells (MDCK), that have been shown to secrete chloride in response to stimulation by mediators of the cyclic AMP signal transduction pathway [4].

When seeded within a collagen matrix, MDCK cells will propagate to form a cyst consisting of a single layer of cells surrounding a fluid-filled cavity containing a slightly hypertonic solution of NaCl [5–7]. In that polarized layer of cells, the apical cell membranes line the cavity and the basolateral membranes are in contact with the collagen matrix. The cystic epithelium resembles that of renal tubules *in vitro* and offer some unique experimental advantages for the study of transepithelial transport systems. Cysts formed by this subcultured strain of cells will secrete fluid in the presence of secretagogues; in the absence of these agents, the cysts will absorb fluid.

A variety of adenylate cyclase agonists and analogues of cAMP stimulate the growth of these cysts [6–8]. These same agents stimulate fluid secretion by monolayers formed by cells of the same cell line [8, 9]. It has been known for some time that MDCK cells can be induced to secrete chloride by adenylate cyclase agonists [4, 10, 11], and it has been suspected that the active secretion of chloride drives fluid secretion as it does in many other secretory epithelia. Studies of fluid secretion and chloride transport in single cysts have provided support for this hypothesis [12, 13].

Arginine vasopressin (AVP) induces the secretion of an hyperosmotic fluid by monolayers of MDCK cells [9] but it has no effect on the low water permeability of the cyst or the monolayer [9, 14]. The secreted fluid has a high concentration of chloride [7] and secretion is inhibited by bumetanide [9]. Cellular levels of cAMP are increased by AVP and fluid secretion is augmented by inhibitors of phosphodiesterase such as 3-isobutyl-1-methyl-xanthine (IBMX) [9].

The methods we have devised to investigate the solute transport mechanisms involved in fluid secretion generated by AVP allow us to couple measurement of transepithelial water flow by the intact cystic epithelium to the measurement of changes in cell volume and in membrane electrical potential that occur as the net transepithelial fluid and solute fluxes are

Received for publication September 22, 1993
and in revised form December 8, 1993
Accepted for publication December 9, 1993

altered. The results obtained indicate that the application of AVP and IBMX reverses the direction of those fluxes from absorption to secretion. The changes in solute fluxes that occur across the apical and basolateral membranes, when the direction of net transepithelial solute flux is reversed, are revealed by the changes in cell volume and membrane potential that result when secretion is activated and when it is blocked by barium and by bumetanide.

Methods

The methods used to culture MDCK cells in our laboratory have been described in detail [6]. MDCK cells were originally obtained from American Type Culture Collection. A subculture of these cells was maintained in plastic dishes in a 1:1 mixture of DME and F12 containing 5% fetal bovine serum (FBS), 10 mM N-hydroxyethylpiperazine-N'-2-ethanesulfonic acid (HEPES), 24 mM sodium bicarbonate, 100 IU/ml of penicillin G, and 0.1 mg/ml of streptomycin. The methods used to obtain cysts have also been described previously [6]. Suspensions of single MDCK cells were dispersed in ice-cold Type I collagen (Vitrogen: Collagen Corp. Palo Alto, California, USA) and placed in a 24-well culture plate. After polymerization, 0.5 ml of serum-free incubation media (1:1 mixture of DME and F12) containing 12.5 ng/ml EGF and 10^{-5} M forskolin were added above the gelled matrix. This combination of EGF and forskolin was found to increase the height of the epithelial cell layer which was advantageous for the epifluorescent measurements (see below). The plates were incubated in an atmosphere of 5% CO_2 in room air at 37°C. Medium was replaced every two to three days, and the cysts were inspected by light microscopy at periodic intervals.

Five to seven days were allowed for cyst growth and then medium without EGF and forskolin was added so that cyst growth and fluid secretion ceased. The gel matrix containing the cysts were removed for dissection 24 hours later. Single cysts were dissected from the matrix using a dissection microscope, a small scalpel and fine forceps. A thin layer of collagen matrix, adhering to the cyst wall, was left in place since removal of collagen has been shown to cause reversal of polarity [15]. The criteria for selection of cysts were spherical form, uniform cell height, and appropriate size. Three or more cysts were transferred from the dissecting dish with the use of a Pasteur pipet and placed in a thermostatted chamber on the stage of an inverted microscope. The cysts were again examined at a magnification of 400× and the same selection criteria were used to select one for study (Fig. 1).

The superfusion chamber consisted of a slit cut into a lucite disc 0.5 cm thick. The floor of the chamber was made by attaching a microscope cover slip to the disc. The tips of two micropipets mounted in micro-manipulators were placed in the solution and attached to the thin rim of collagen gel surrounding the cyst. The chamber temperature was maintained at 37°C and its 0.5 ml volume was constantly exchanged at a rate of 3 ml/min. A gentle jet of gas (3% CO_2, 97% O_2) was directed over the bathing fluid. The pH of the bath in the chamber was monitored in some experiments with small-diameter electrodes immersed within the chamber.

Measurement of fluid secretion rate and cell volume

The fluid secretion rate was determined from the rate of change in cyst cavity volume. Cavity volume was measured in the following manner: We focused on the equatorial plane of the spherical cyst using a 40× fluor objective (Nikon, Garden City, New York, USA) and periodically recorded the image on video tape using a video camera (RCA TC 1005/U, Lancaster, Pennsylvania, USA) and a VCR (JVC CR-6060U, Maspeth, New York, USA). The camera was attached to a multi-image module (Nikon) that was connected to the side port of the microscope (Nikon Diaphot). In most experiments fluorescence measurements were also made. To prevent excitation of the dye by the tungsten illuminating microscope lamp, its light was passed through a cut-on filter (600 nm). After passing through the objective, the light was directed to the video camera by a dichroic mirror in the multi-image module. For each recording of the image, a computer (386/25 mHz) turned on the tungsten lamp and the VCR for a five second period. Images were recorded at two to three minute intervals (Fig. 1A).

A video analysis system (Jandel JAVA, Corte Madera, California, USA), installed in the computer, was used to process the videotaped images. The system enhanced the contrast of the image, automatically traced the border of the cyst cavity and calculated the planar area enclosed within that border (Fig. 1B). The computer then calculated the fluid volume within the cavity and the area of the surface lining the cavity using standard geometric equations based on the assumption that the cavity is a sphere. The fluid secretion rate was calculated from the slope of the regression line fitting the plot of cavity volume versus time (Fig. 2). To normalize the measurements among experiments, fluid secretion rate was expressed in units of volume per unit time per cm^2 of the calculated surface area of the cavity at the beginning of each control or experimental period. To determine cell volume, the video analysis system was also used to trace the outer border of the cyst and determine total cyst volume. The cavity volume was subtracted from that to obtain cell volume. To determine the degree of reproducibility of the these measurements, 10 measurements of the cavity volume of the cyst in Figure 1A were made. The mean volume was 195.33 pl with a range of 195.19 to 195.50. The standard deviation of the measurements = 0.056% of the mean. Ten measurements of the cell volume yielded a mean of 178.30 pl with a range of 177.39 to 179.09. The standard deviation of the measurements = 0.32% of the mean.

Fluorescence measurements

Measurements of epi-fluorescence were used to record changes in membrane potential and to measure cell pH. The lipophilic anion, bis-oxonol [bis-(1,3-diethylbarbiturate) trimethine oxonol; Molecular Probes, Eugene, Oregon, USA] was used for the former purpose. The accumulation of this dye within the cell membrane is potential-dependent; depolarization increases the concentration within the membrane and polarization drives the dye out. In addition the association of the dye with the membrane greatly enhances its fluorescence quantum efficiency [16]. It has been shown that this anionic dye is largely excluded from the cytoplasm of lymphocytes and, unlike the cationic voltage-sensitive cyanine dyes, is also excluded from mitochondria [17]. This dye was added to the bathing solutions

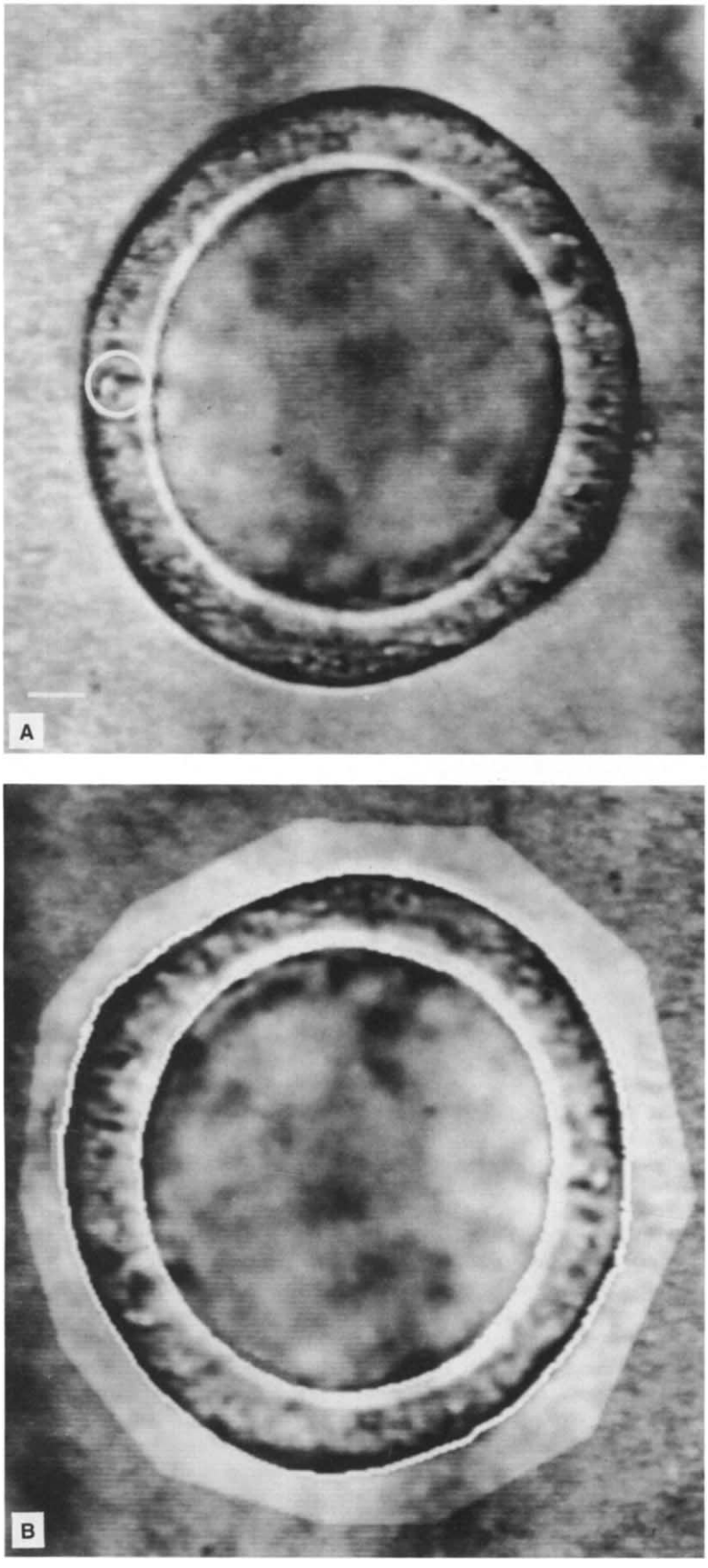

Fig. 1. A. *Video image of MDCK cyst.* The circle indicates the region from which fluorescence was recorded. The bar = 10 μm. **B.** The same image after processing by the image analysis system. The white lines are the automatic tracing of the inner cavity surface and the outer cyst surface. The areas within the circles were calculated by the analysis system from which the cavity volume and total cyst volume were derived. The difference between the two equaled cell volume.

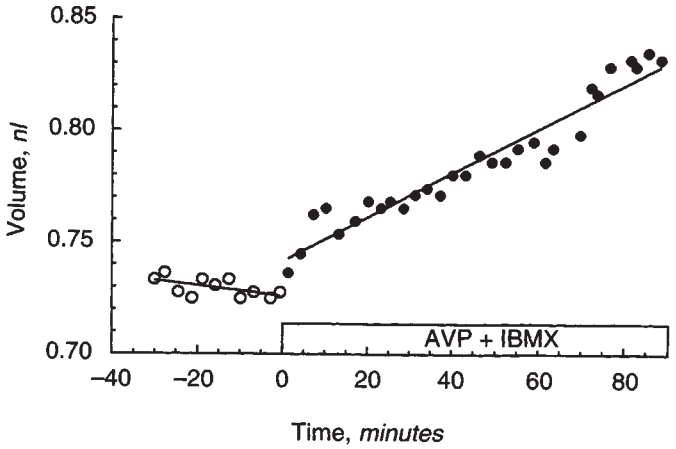

Fig. 2. *The change in cavity volume induced by 10 mU/ml AVP and 0.1 mM IBMX.* The solid lines are regression lines. See text for values.

at a concentration of 200 nM. The fluorophor was excited at a wavelength of 540 nm and fluorescence emission was measured at a wavelength of 580 nm.

A Xenon arc lamp (75 watt) was used to provide the exciting light. That light passed through, in sequence, a computer controlled shutter, a bandpass filter (540 nm, Omega Optical, Brattleboro, Vermont, USA) mounted in a motor driven and computer controlled filter wheel (Eastern Microscope, Raleigh, North Carolina, USA), a 2.0 optical density filter (to reduce light intensity) to a dichroic mirror (565 nm) which directed the light through a 40× fluor objective (Nikon) to the tissue. The light emitted by the dye passed back through the objective and the dichroic mirror to the multi-image module in which another dichroic mirror (595 nm) directed it through a bandpass filter (580 nm) to a photometer (Nikon). The output of the photometer passed directly to an analog-digital board (Data Translation Inc., Marlboro, Massachusetts, USA) monitored by the computer. For each measurement the computer opened the shutter for a period of 120 msec, recorded the output of the photometer at 1 msec intervals, averaged those values over the last 100 msec of that period and plotted that value on the computer screen in real time. Computer software for this procedure was developed in this laboratory.

The cyst was positioned so that light from a cell area on the periphery of the equatorial plane of the cyst passed through a pinhole in the emitted light pathway (Fig. 1A). This recorded light from a cylinder of tissue 11.4 μm in diameter and excluded light from the cyst cavity. The position of the cyst with regard to the pinhole was carefully monitored and maintained throughout each experiment. Background fluorescence was measured before the dye was introduced into the chamber and all subsequent readings were corrected for that. The background averaged less than 1% of the fluorescence recorded during the experiment. The bathing solutions containing the dye were periodically checked for fluorescence and none could be recorded above the background values. The dye did not accumulate in the collagen layer surrounding the cyst.

Calibration of the dye readings in terms of millivolts was attempted using the ionophore gramicidin D (1.5 μM) and solutions of varying Na^+ concentration [18]. This procedure proved to be impractical. The ionic composition of the fluid within the cyst cavity equilibrates with that of the bathing solution at a slow rate. Thus each change of the calibration solution established ionic gradients between the bath and the cavity. This resulted in a relatively slow drift of the photometer reading which we attribute to paracellular current flow altering the membrane potentials. Thus we have chosen to express the data in terms of an experimental to control ratio of the photometer readings. This allowed us to record the relative changes that occurred in membrane potential in each experiment. To test the efficacy of this technique, we measured the effect of 1 mM barium in seven cysts not stimulated to secrete fluid. Barium caused the photometer readings to increase, signifying depolarization of the cells. The experimental to control ratio averaged 1.183 ± 0.036, $P < 0.005$. We also found that increasing the potassium concentration from 5 to 25 mM (the sodium concentration was reduced 20 mM) increased the ratio to 1.087 ± 0.030 ($N = 7$, $P < 0.05$). However, this maneuver also established ionic gradients and current flow between the cavity and the bath.

Cell pH was measured with the use of 2'7'-bis(carboxyethyl)-5[6]-carboxyfluorescein (BCECF, Molecular Probes, Eugene, Oregon, USA) as described previously [19]. The cyst cells were loaded with the dye by exposing them to 10 μM of the acetoxymethyl ester of the dye (BCECF-AM) for 15 minutes. BCECF leaked from the cells at a significant rate so in some experiments 0.5 μM BCECF-AM was included in the chamber perfusate after the loading period. The equipment setup described above was used in the measurements. The dye was excited alternately with light at wavelengths of 440 and 495 nm and the intensity of the emitted light at a wavelength of 535 nm was measured. The ratio of the emission intensity obtained with the two exciting wavelengths (495/440) was calculated. The ratio values were calibrated in terms of pH units using the nigericin-high potassium technique described previously [19].

The thin layer of collagen gel surrounding the isolated cyst could act as a diffusion barrier between the cyst and the bathing media. To evaluate this, we measured the rate of washout of fluorescein from the gel using the epifluorescence methods described above and earlier [20]. We positioned the cyst so that the photometer recorded light from a circle of gel 4.56 μm in diameter tangential to the equatorial plane of the cyst. We also recorded light from the bathing solution at a spot in the same focus plane adjacent to the gel layer. The chamber was perfused with a solution containing 50 μM fluorescein at a rate of 3.2 ml/min until the fluorescence from the gel reached a steady state. That perfusion line was then closed, and a second line containing control solution was opened (0 time for the washout recordings). The chamber was partially drained twice via a suction line in rapid succession to facilitate the exchange of the chamber solution. This was the procedure used in all experiments. Dye readings were obtained at short intervals (~5 sec). In the first test, two measurements of gel washout and one measurement of chamber washout were made. The gel measurements were made at spots with a horizontal distance of 47.5 and 64.5 μm from the gel edge. The half-times for washout were 13.9 and 13.1 seconds, respectively; the half-time for the chamber washout was 11.9 seconds. In a second test using a different cyst, three measurements were made at distances from the collagen edge of 29.8, 35.2 and 49.6 μm. The half-times for

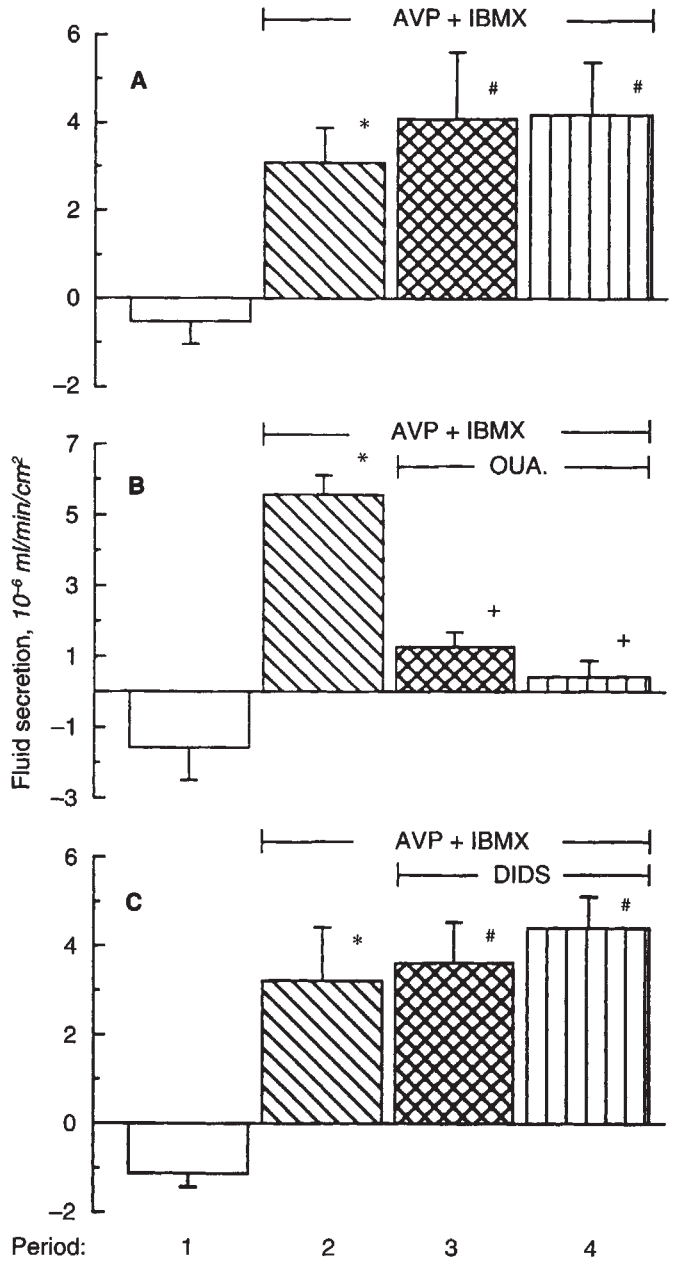

Fig. 3. A. *Fluid secretion rates induced by 10 mU/ml AVP and 0.1 mM IBMX. N = 6.* **B.** The effect of 0.1 mM ouabain on secretion induced by AVP and IBMX. $N = 4$. **C.** The effect of 0.1 mM DIDS on secretion induced by AVP and IBMX. $N = 4$. Each bar represents a 30 minute period. *Difference between periods 1 and 2, $P < 0.05$. #Differences between periods 2 and 3 and between 2 and 4, NS. +Differences between periods 2 and 3 and between 2 and 4, $P < 0.05$.

gel washout were 9.4, 9.7 and 9.8 seconds, respectively. The half-time for chamber washout was 8.7 seconds. It is evident that the gel rapidly equilibrated with the bathing solution. The small amount of time involved should not have affected the measurements reported below.

Solutions

The solution used to superfuse the cysts consisted of 147 mM Na^+, 119 mM Cl^-, 5 mM K^+, 20 mM HCO_3^-, 2 mM Ca^{2+}, 1.2 mM Mg^{2+}, 1.2 mM SO_4^{2-}, 2.5 mM HPO_4^{2-}, 5 mM glucose, 5 mM acetate, 1 mM citrate, 4 mM lactate, 0.5 mM butyrate, 6 mM alanine and 9.9 mM raffinose. The raffinose was used to raise the osmolality of the solution to that of the incubation media, 312 mOsm/kg H_2O. Initially we equilibrated the solution with 5% CO_2, 95% O_2. However, measurements of cell pH indicated that cell pH equaled 7.02. We then used 3% CO_2, 97% O_2, in all subsequent experiments in order to increase cell pH. The composition of the solution used during dissection of the cysts from the gel was the same except that it also contained 5% bovine serum albumin. Fluid secretion was initiated by adding 10 mU/ml AVP and 0.1 mM IBMX to the superfusate.

Statistics

Both control and experimental measurements were made in the same cyst. Repeated measures analysis of variance and the Student-Newman-Keuls test were used to determine significance of changes. These statistical tests were applied to absolute values for fluid secretion, cell volume and bis-oxonol fluorescence rather than to E/C ratios.

Results

Effect of ouabain and DIDS on fluid secretion

Initial experiments tested the effect of AVP + IBMX on net fluid transport by the cysts. A control period of 30 minutes was followed by an experimental period of 90 minutes during which the superfusate contained AVP and IBMX. The results of one such experiment is presented in Figure 2. Each point represents a separate measurement of cyst cavity volume and the lines are the regression lines for the two periods. The slopes of the regression lines equal the fluid secretion rate. Fluid absorption was evident in the control period (the fluid transport rate equaled -2.13×10^{-4} nl/min, $r = 0.55$) and secretion occurred in the experimental period after application of AVP and IBMX (9.88×10^{-4} nl/min, $r = 0.96$) in the experimental period. The initial diameter of the cyst cavity was 111.5 μm and the cavity surface area was 3.91×10^{-4} cm². The respective fluid transport rates, expressed in terms of that surface area, were −0.54 and 2.53×10^{-6} ml/min/cm². The results for six such experiments are presented in Figure 3A. For purposes of comparison with subsequent experiments the experimental period was subdivided into three 30-minute periods. The rate of secretion did not differ among those three periods.

To determine if Na-K-ATPase may be involved in the process of fluid secretion, we tested the effect of 0.1 mM ouabain on the secretion induced by AVP and IBMX in four experiments (Fig. 3B). After the control period in which no net secretion of fluid occurred, AVP and IBMX were administered and the secretion rate for the first experimental period of 30 minutes averaged $5.57 \pm 0.55 \times 10^{-6}$ ml/min/cm². Ouabain was then administered together with AVP and IBMX for two subsequent periods. Ouabain greatly reduced fluid secretion in those two periods.

It has been suggested that Cl-HCO_3 exchange in the basolateral membrane may be a primary transport system involved in fluid secretion [12, 13]. Accordingly, the effect of the inhibitor, diisothiocyanatostilbene-2,2'-disulfonic acid (DIDS), was tested in four experiments using the same protocol as described above for ouabain. In the control period, net reabsorption of fluid occurred. In the first experimental period AVP and IBMX

Table 1. Cell pH before and during fluid secretion

Experiment no.	Secretion rate $\times 10^{-6}$ ml/min/cm^2		Cell pH	
	Control	Exper.	Control	Exper.
1	0.36	6.42	7.05	7.07
2	−1.82	8.92	6.96	6.99
3	0.45	4.98	7.14	7.07
4	0.18	8.15	7.22	7.20

Cell pH values are averages of 10+ readings taken throughout each period. Fluid secretion was initiated in Exps. 1 to 3 by 10 μM forskolin + 0.1 mM IBMX. In Exp. 4 AVP and IBMX was used. The bath solution buffer was 20 mM $NaHCO_3$ + 5% CO_2; pH = 7.40.

Table 2. Fluid secretion, cell volume and membrane potential changes following initiation of secretion with AVP and IBMX

Fluid secretion rate $\times 10^{-6}$ ml/min/cm^2	
Control	−0.83 ± 0.34[a]
AVP + IBMX	4.24 ± 0.49
Difference	5.07 ± 0.65[b]
Cell volume changes	
E/C	
4–6 min	0.926 ± 0.005[b]
20 min	0.921 ± 0.007[b]
Membrane potential changes	
E/C bis-oxonol fluorescence	
1 min	0.998 ± 0.013
5 min	0.994 ± 0.019
20 min	0.981 ± 0.031

N = 23. All values are means ± SE. Fluid secretion rate and cell volume are expressed as per cm^2 inner surface area.
[a] $P < 0.025$
[b] $P < 0.05$

alone induced fluid secretion at a rate of 3.21 ± 1.19 × 10^{-6} ml/min/cm^2. In the subsequent periods in which 0.1 mM DIDS was administered, the secretion rate did not change significantly; it averaged 3.60 ± 0.92 and 4.39 ± 0.72 × 10^{-6} ml/min/cm^2 in those two periods.

Cell pH

To determine if a mechanism that alters cell pH is involved in fluid secretion, we measured cell pH in four experiments (Table 1). The average pH in the control and experimental periods did not differ (Exp. − Cont. = −0.01 ± 0.02). No discernable trend or apparent transient changes in pH were recorded during the experimental period.

Cell volume and membrane potential changes during secretion

In all subsequent experiments cavity volume, cell volume and bis-oxonol fluorescence were measured in four sequential 20 minute periods: Period 1, control period; Period 2, the cyst was exposed to AVP + IBMX; Period 3, a drug was administered together with AVP and IBMX; Period 4, recovery period in which AVP and IBMX alone were administered.

Table 2 lists the values for net fluid movement in the control period (Period 1) and the changes that occurred when the cysts were initially exposed to AVP and IBMX (Period 2) in 23 cysts. In the control period 17 of the cysts exhibited net fluid reabsorption (negative secretion). AVP and IBMX stimulated fluid secretion in all the cysts. The changes that occurred in cell volume (Exp/Cont) and membrane potential (Exp/Cont bis-oxonol fluorescence) following the administration of AVP and IBMX are also presented in Table 2. The control cell volume averaged 1.76 × 10^{-3} ml/cm^2 inner surface area. The initiation of secretion was accompanied by a loss of cell volume of 7.9% for the entire period (20 min); 93% of that loss occurred within the first four to six minutes of secretion (see Fig. 5 for example). No significant changes occurred in membrane potential. However, the mean values mask large changes in individual experiments. The changes that occurred in all 23 experiments are shown in Figure 4. In 13 experiments significant hyperpolarization occurred (E/C = 0.80 − 0.94 at 20 min). In six experiments marked depolarization occurred (E/C = 1.112 − 1.305 at 20 min). These cysts also differed in their fluid transport rates. The cysts that depolarized transported fluid at greater rates both in the control period (−1.71 ± 0.54 vs. −0.13 ± 0.46 × 10^{-6} ml/min/cm^2, $P < 0.001$) and in the experimental period (5.28 ± 1.09 vs 3.77 ± 0.63 × 10^{-6} ml/min/cm^2, $P < 0.005$) than did those that hyperpolarized. These results suggest that these two groups of cysts differed in factors that participate in both reabsorption and secretion of fluid, such as Na-K-ATPase activity or the magnitude of the control membrane potentials. We do not believe that these differences reflect a variation in cell type; rather, they simply represent experimental variations among a single population of cysts.

Effect of basolateral membrane depolarization

To determine if membrane electrical gradients played a role in fluid secretion, we applied 1 mM barium to the cyst after secretion was initiated by AVP and IBMX. The results of one such experiment are presented in Figure 5. Measurement of cavity volume indicated that no net fluid transport occurred in the control period (Fig. 5A). The application of AVP and IBMX initiated fluid secretion at a rate of 7.2 × 10^{-6} ml/min/cm^2. The addition of 1 mM barium in the presence of AVP and IBMX completely blocked secretion. This effect was reversed when barium was removed. Cell volume (Fig. 5B) fell to 89.9% of control in response to AVP and IBMX. In the presence of barium, cell volume transiently increased to 94% of control and then gradually fell. The addition of the secretagogues caused a fall in bis-oxonol fluorescence (Fig. 5C) indicating membrane hyperpolarization. This also was reversed by barium.

The data for six such experiments are summarized in Figure 6. The mean rates of fluid secretion are presented in the top panel. Barium completely inhibited the fluid secretion induced by AVP and IBMX and the effect was rapidly and completely reversible. AVP and IBMX reduced cell volume to 91.8 ± 0.8%; barium caused a transient increase to 94.3 ± 0.07%. In this series of experiments, bis-oxonol fluorescence intensity fell to 87.6 ± 2.3% of control when AVP and IBMX were applied to the cysts, indicating that the initiation of secretion was accompanied by membrane hyperpolarization. (This subset of experiments are included within the series illustrated in Fig. 4). The application of barium in the presence of AVP and IBMX caused fluorescence intensity to rise to 107 ± 3%, indicating depolarization. Membrane repolarization occurred following the removal of barium.

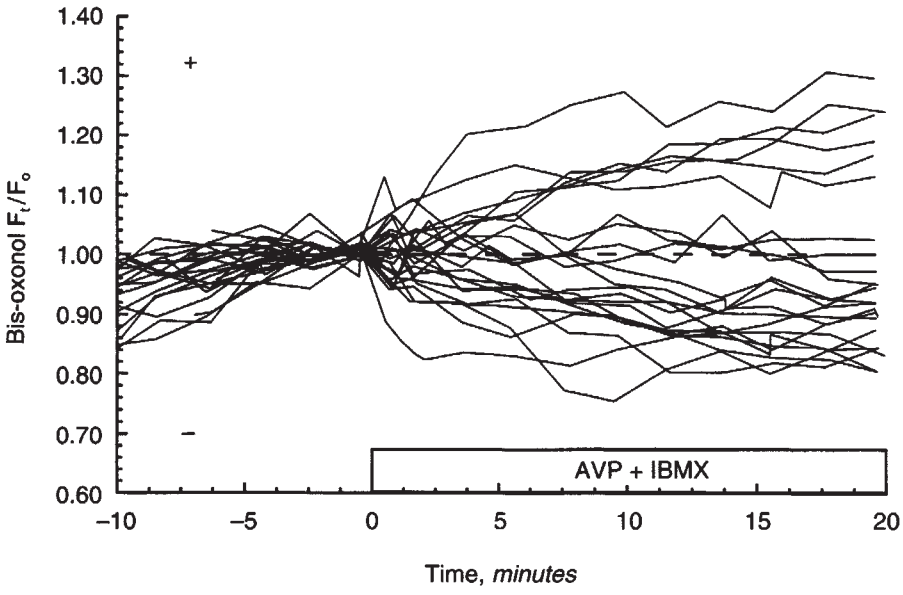

Fig. 4. *Membrane potential changes following induction of secretion by 10 mU/ml AVP and 0.1 mM IBMX.* F_t/F_o = bis-oxonol fluorescence at time t/fluorescence at time 0. A reduction in the ratio value indicates hyperpolarization (−) and a rise in the ratio indicates hypopolarization (+). The dashed line indicates a ratio value of 1. See Table 2 for statistical summary.

Effect of bumetanide

Bumetanide was used to determine if Na-Cl or Na-K-2Cl cotransport has a role in fluid secretion. The results of one experiment in which 100 μM bumetanide was used are illustrated in Figure 7. The secretagogues initiated a fluid secretion rate of 2.32×10^{-6} ml/min/cm^2 (Fig. 7A). This was completely inhibited by bumetanide and the inhibition was reversed by the removal of the drug. Cell volume (Fig. 7B) fell to 95.3% of the control level upon initiation of secretion; bumetanide induced an additional fall to 90.8% of control. In this experiment the onset of secretion was accompanied by a rise in fluorescence intensity to 111% of control (depolarization). Bumetanide rapidly and drastically reversed this to 66% of control (hyperpolarization). Removal of bumetanide returned the fluorescence intensity to the control level.

A summary of the results of six experiments with 100 μM bumetanide is presented in Table 3 (Series I). Secretion was completely inhibited by the drug and this was partially reversed when it was removed. The secretion-induced fall in cell volume was augmented by the drug. Bis-oxonol fluorescence intensity was not altered significantly by AVP and IBMX in this series of experiments but the inhibitor caused a significant reduction (hyperpolarization).

A smaller concentration of bumetanide, 10 μM, was used in four experiments (Series II in Table 3). At this concentration, the inhibitor significantly reduced fluid secretion but to a lesser extent than occurred with 100 μM. Cell volume fell in each experiment but the decrease was too small to be significant (−1.1 ± 0.3%). The same was true for bis-oxonol fluorescence (−12.0 ± 0.4%).

To determine if the transport mechanism or mechanisms inhibited by bumetanide were active in the control state, we applied 100 μM bumetanide to cysts that had not been exposed to a secretagogue for 24 hours. The results of five experiments are presented in Table 3 (Series III). Net fluid absorption occurred in the control period ($P < 0.02$). That was not affected by application of bumetanide and no significant changes occurred in cell volume or in bis-oxonol fluorescence.

Discussion

The MDCK cyst

Cysts have been shown to develop by clonal growth from MDCK cells seeded in collagen matrix [5]; thus, this method of culture selects cells from the wild strain of MDCK cells (American Type Culture Collection) that are capable of secreting solutes and water. Studies of the morphology of the MDCK cyst grown in collagen have shown that the organization of the epithelium and the orientation of the membranes and the tight junction closely resemble that of distal nephron structures. The structural polarization is mirrored by the functional polarization of membrane proteins including basolateral Na-K-ATPase, apical gp135, lateral membrane uvomorulin and tight junction ZO-1 [21]. Cyst enlargement is enhanced by agents that promote fluid secretion in monolayers of the same cell line, agents that activate adenylate cyclase and analogs of cAMP [6–8]. The secreted fluid has a NaCl composition similar to that of the culture medium and is slightly hypertonic [5–7]. The hydraulic conductivity of the cystic epithelium (P_f) is low, 6.8 μm/second, a value similar to that of medullary and cortical thick ascending limbs of Henle and is not altered by AVP, IBMX or 8-Br-cAMP. The reflection coefficient of the cystic epithelium for NaCl is indistinguishable from 1.0 [22]. Thus the cultured cyst presents a phenotype of an organized epithelium that closely resembles the behavior of segments of the distal renal tubule studied *in vitro* [1]. As such it offers several advantages as an experimental tool for the study of transepithelial transport processes and their control.

Techniques

The video techniques we have used to measure the rate of fluid secretion and cell volume are a modification of those used

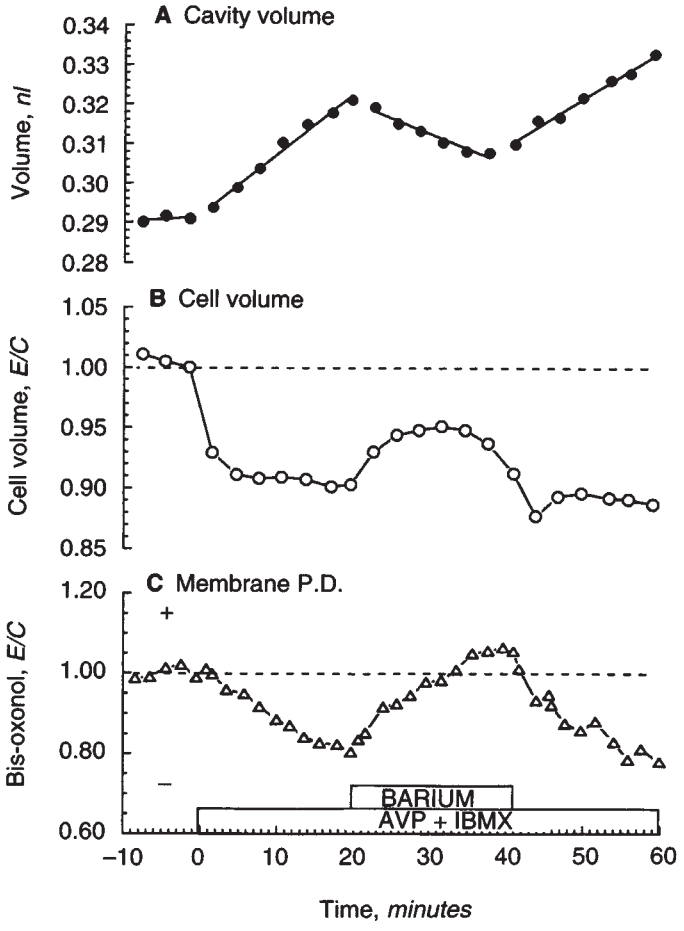

Fig. 5. *The effect of 1 mM barium on cavity volume, cell volume and membrane potential following the induction of secretion by 10 mU/ml AVP and 0.1 mM IBMX.* E/C = experimental/control. The solid lines in the upper panel are regression lines for each period and were used to calculate fluid secretion rates. The secretion rates for each of the four periods were 0.24, 7.20, −3.37, and 5.45 × 10^{-6} ml/min/cm^2 cavity surface area. The dashed lines in the second and third panel = an experimental/control ratio value of 1.00. The control cell volume = 1.10 × 10^{-3} ml/cm^2 outer surface area. The control bis-oxonol fluorescence = 158 photometer units. A fall in the ratio for bis-oxonol fluorescence indicates hyperpolarization; a rise indicates membrane depolarization.

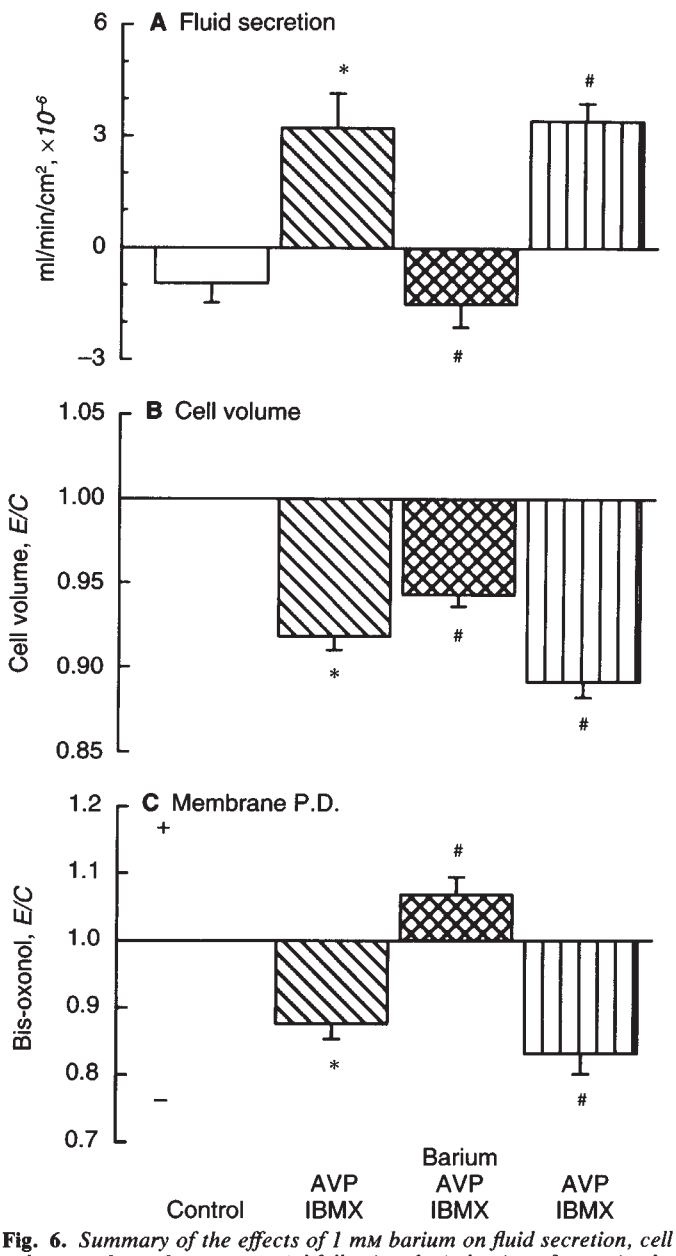

Fig. 6. *Summary of the effects of 1 mM barium on fluid secretion, cell volume and membrane potential following the induction of secretion by 10 mU/ml AVP and 0.1 mM IBMX.* * Comparison with control period, $P < 0.05$. # Comparison with preceding period, $P < 0.05$.

by Tanner, Maxwell and McAteer [12]. The measurements are based on the assumption that the cyst is a sphere and that the cell layer has a uniform height. Spherical form and uniform cell height in basal medium were criteria for selection of the cysts to be studied. We found that measurements of cavity volume at three minute intervals over a 20 minute period provided a solid indication of the net rate of fluid transport (Figs. 5 and 7). The secretion rate over a 90 minute period was stable (Figs. 2 and 3). This and the rapid rate of change in the direction of net transport induced by the secretagogues and inhibitors we used (Figs. 5 and 7) permitted control and sequential experimental measurements to be made in each cyst. Small changes in cell volume were reproducibly detected.

Cysts grown in collagen with fetal calf serum or forskolin obviously secrete fluid [6–8]. EGF, which causes hypertrophy of MDCK cells (unpublished observations), was added to the medium to increase cell height during the initiation of the cyst and thereby increase the volume of tissue from which epifluorescence was recorded (Fig. 1). We removed EGF and secretagogues for 24 hours prior to study to enhance changes with applied experimental agents. This revealed that these cells can reabsorb fluid, and presumably solutes, when the secretory processes are not stimulated, a finding in keeping with previous measurements in planar monolayers of MDCK cells [9].

The epifluorimetric techniques we used are similar to those that we and others have applied to isolated renal tubules. Bis-oxonol has been used to measure cell membrane potentials in suspensions of MDCK cells and in glomerular mesangial cells

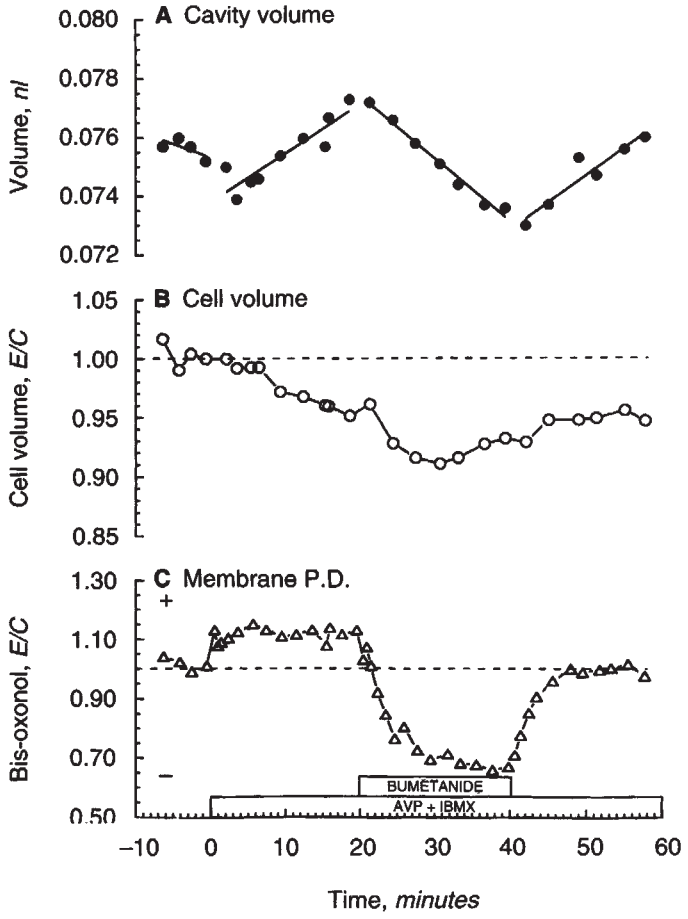

Fig. 7. *The effects of 100 μM bumetanide on cavity volume (●), cell volume (○) and membrane potential (△) following the induction of secretion by 10 mU/ml AVP and 0.1 mM IBMX.* The fluid secretion rates for each of the four periods were −1.04, 2.32, −2.39 and 2.12 × 10^{-6} ml/min/cm² cavity surface area. The control cell volume was 0.75 × 10^{-3} ml/cm² outer surface area. The control bis-oxonol fluorescence = 148 photometer units. See Fig. 5 for details of figure.

Table 3. Effect of bumetanide

	Secretion rate × 10^{-6} ml/min/cm²	Cell volume	Bis-oxonol
		E/C	
Series I, $N = 6$			
Control	−1.36 ± 0.70		
AVP + IBMX	4.49 ± 1.23[a]	0.92 ± 0.01[a]	1.14 ± 0.06
AVP + IBMX + 100 μM Bumet	−0.75 ± 0.55[b]	0.88 ± 0.02[b]	0.86 ± 0.08[b]
AVP + IBMX	1.74 ± 0.66	0.92 ± 0.01	1.01 ± 0.07
Series II, $N = 4$			
Control	−1.87 ± 0.57		
AVP + IBMX	2.86 ± 0.48[a]	0.93 ± 0.01[a]	1.11 ± 0.09
AVP + IBMX + 10 μM Bumet	0.48 ± 0.53[b]	0.92 ± 0.01	0.99 ± 0.07
AVP + IBMX	1.25 ± 0.63	0.93 ± 0.01	0.96 ± 0.09
Series III, $N = 5$			
Control	−1.75 ± 0.39		
100 μM Bumet	−1.87 ± 0.47	0.97 ± 0.01	0.98 ± 0.07

[a] Comparison to control period: $P < 0.05$
[b] Comparison to 2nd period $P < 0.05$

[23, 24]. We found that the dye provided reproducible measurements of the direction and relative magnitude of the changes in membrane potential. The extent to which the dye entered the apical membrane and the contribution of that membrane potential to the recorded changes could not be ascertained. Macias et al measured the transepithelial PD of MDCK cysts formed by cells of two different strains with the use of microelectrodes. The control PD averaged −1.8 and −2.0 mV and dibutyryl cAMP + IBMX increased this to −5.6 and −7.8 mV [25]. These differences in the PDs of the apical and basolateral membranes can be affected by events occurring at either membrane. In addition, since the two membranes are electrically coupled via the paracellular pathway, a change in the PD of one membrane alters the PD of the other membrane. Thus interpretation of the changes in bis-oxonol fluorescence must be interpreted with the same caution applied to measurements of transepithelial PD. Calibration of the dye readings in terms of millivolts is difficult because of the problems involved in making sequential changes in the composition of the fluid in the cyst cavity (see **Methods**).

The coupling of measurements of cell volume and changes in membrane potential to measurements of fluid secretion permitted us to follow changes in cell function as secretion was initiated or inhibited. Thus we were able to show that cell volume was rapidly reduced when secretion was initiated and remained low as long as the rate of fluid secretion remained stable. No evidence of a regulatory volume increase occurred. Inhibition of secretion by basolateral membrane depolarization was accompanied by a rise in cell volume. Inhibition of secretion by bumetanide was accompanied by an additional fall in cell volume. The data obtained with bis-oxonol indicated that the initiation of secretion by AVP and IBMX was accompanied by variable changes in membrane potential. Depolarization of the membranes inhibited AVP-induced secretion and inhibition of secretion by bumetanide was coupled with membrane hyperpolarization. Neither cell volume nor membrane potential was affected by bumetanide in cysts in the absence of secretagogues.

Conventional model for epithelial fluid secretion

The mechanism of fluid secretion by a variety of epithelia has been shown to be due to transcellular Cl transport. In the tracheal epithelium [26], the salivary gland [27], the shark rectal gland [28] and other secretory epithelia, chloride enters the cell at the basolateral membrane via a Na-Cl or Na-K-2Cl cotransporter in the basolateral membrane driven by the transmembrane sodium gradient established and maintained by Na-K-ATPase located in the basolateral membrane. Chloride exits the cell via a conductance pathway in the apical membrane driven by the electrochemical gradient across that membrane. The depolarizing chloride current across the apical membrane is balanced by a hyperpolarizing potassium current across the basolateral membrane. The paracellular diffusion of Na into the lumen is driven by the transepithelial potential difference (lumen negative). The addition of chloride and sodium to the lumenal fluid results in an osmotic force driving water secretion. Agents that stimulate adenylate cyclase and cAMP analogues typically cause secretion by these epithelia [29, 30].

Secretion is initiated by activation of the apical chloride conductance, the basolateral potassium conductance and the basolateral cotransporter. We consider below that the results reported here, coupled with those reported by other investigators, are consistent with the hypothesis that these mechanisms drive fluid secretion by the MDCK cyst.

Involvement of chloride

Chloride secretion by monolayers of MDCK cells in response to epinephrine, forskolin and prostaglandin E_1 has been reported by Simmons and coworkers [4, 10, 11]. Mangoo-Karim and coworkers reported that the chloride concentration of the cystic fluid exceeded that of the bath [7] and Macias et al found that the transepithelial electrochemical gradient across the cyst wall opposed passive chloride secretion. They also found that, in the absence of secretagogues, the cellular Cl activity, 60 ± 1 mM, exceeded the value that would exist if electrochemical equilibrium for chloride prevailed across both the apical and the basolateral membrane [13]. Thus an electrochemical gradient opposes chloride entry across the basolateral membrane, implying the presence of active inward transport during secretion. The electrochemical gradient across the apical membrane may drive chloride from the cell into the cyst lumen when secretion is initiated. Kolb, Brown and Murer have reported the presence of a chloride channel with a conductance of 460 pS in MDCK cells. The number of open channels was significantly increased by epinephrine which has also been shown to stimulate chloride secretion [31]. Anion channels with a much smaller conductance have been reported to be activated by cell swelling [32, 33].

Effect of barium

Depolarization of the cell by the application of barium inhibited fluid secretion, indicating that membrane electrical gradients are involved in fluid secretion (Figs. 5 and 6). Barium-induced depolarization of the basolateral membrane of the canine tracheal epithelium also inhibited chloride secretion [34], and Greger and Schlatter found that barium inhibited active secretion by the shark rectal gland and that the depolarization reduced the electrochemical gradient for chloride efflux [35]. They also reported that intracellular activities of K and Cl increased. We found that cell volume increased after application of barium, indicative of an increase in total cell solutes. Thus it seems reasonable to conclude that barium blocked the potassium conductance of the basolateral membrane and the ensuing depolarization of the cell reduced the force for chloride efflux across the apical membrane resulting in inhibition of fluid secretion. The retention of potassium and chloride in the cell led to cell swelling.

Effect of bumetanide

Bumetanide, an inhibitor of Na-K-2Cl cotransport, abolished fluid secretion, hyperpolarized the cell membranes and caused an additional loss of cell volume. These results compare closely to those obtained with the use of furosemide, another inhibitor of Na-K-2Cl cotransport, in the mammalian thick ascending limb of the loop of Henle [36], the shark rectal gland [35] and the shark renal proximal tubule [37]. Greger and Schlatter found that furosemide reduced Cl activity in the cells of the shark rectal gland to the level expected for passive distribution of Cl across the cell membrane, caused a small decrease in cell potassium activity and hyperpolarized the basolateral membrane [35]. In the mouse thick ascending limb, transepithelial chloride transport occurs in the opposite direction, from apex to base. However the same transport mechanisms as those in the shark rectal gland are responsible for this chloride transport and it is stimulated by AVP [38]. In that tissue furosemide also inhibited chloride transport and hyperpolarized the cell membranes [36]. It is reasonable to conclude that in our experiments bumetanide inhibited Na-Cl or Na-K-2Cl cotransport. The ensuing fall in cell chloride activity reduced the depolarizing current across the apical membrane, resulting in hyperpolarization of the cell membranes. The fall in cell chloride activity and the partial inhibition of potassium entry into the cell caused additional cell shrinkage.

In a study of fluid secretion by MDCK cysts, Tanner and associates obtained evidence which they have interpreted to indicate that, in cysts stimulated to secrete fluid, chloride enters the cell across the basolateral membrane via Cl-HCO_3 exchange [12]. We interpret the data reported herein to indicate that the mechanism of entry is a Na-Cl or Na-K-2Cl cotransporter. Tanner et al reported that the fluid secretion rate in MDCK cysts was 23% less in the presence of 10 μM bumetanide, an inhibitor of the cotransporter; however, this effect was not statistically significant. In their experiments control and experimental measurements were made in separate groups of cysts. We found that the same concentration of bumetanide reduced fluid secretion 83% in experiments in which paired control and experimental measurements were made on the same cyst (Table 3). Tanner et al also found that fluid secretion induced by exposure of cysts to AVP was inhibited if the cysts were pretreated with 0.1 mM DIDS for 90 minutes. DIDS was removed when the secretagogue was added. In our paired experiments, we exposed the cysts to AVP + IBMX for 30 minutes, and then to AVP + IBMX + 0.1 mM DIDS for 60 minutes. The addition of DIDS had no effect on the rate of secretion (Fig. 3). Tanner et al also reported that the nominal absence of HCO_3/CO_2 from the bathing solution plus the presence of acetazolamide prevented stimulation of fluid secretion. Pretreatment with amiloride also inhibited secretion. Macias et al reported that furosemide caused only a transient hyperpolarization of the basolateral membrane and no change in cell chloride activity in MDCK cysts not stimulated to secrete fluid [13]. They also reported that reduction of bath Na did not reduce cell chloride activity but that an increase in bath HCO_3 concentration to 50 mM did in cysts in the absence of secretagogues. These results were also interpreted to indicate that Cl/HCO_3 exchange is the mechanism of chloride entry into the cell during secretion.

Our results are not consistent with the idea that a Cl/HCO_3 exchanger is the major mechanism of chloride entry into the cell when the cyst is secreting fluid. Stimulation of secretion was not accompanied by a change in cell pH (Table 1) as might be predicted if the secretagogue-induced exit of chloride across the apical membrane increased Cl/HCO_3 exchange at the basolateral membrane. DIDS was without effect in our experiments when it was applied after secretion was initiated (Fig. 3). Low (10 μM) and high (100 μM) concentrations of bumetanide did inhibit secretion and the inhibition with the high concentration was associated with a fall in cell volume, an effect not expected to occur if an antiport mechanism was inhibited or if the high

concentration somehow blocked the apical conductance. We did find that 100 uM bumetanide had no effect on cell volume, membrane potentials and net fluid transport in the absence of a secretagogue (Table 3).

This last finding may explain the discrepancy between our results and those of Tanner et al [12] and Macias et al [13]. We suggest that, in the absence of secretagogues, the Cl/HCO_3 exchanger may play a major role in maintaining a high cell chloride concentration in the MDCK cell. Secretion may be inhibited if that exchange is blocked prior to the application of certain secretagogues. However, the secretagogues used in the present study activate Na-K-2Cl cotransport and during secretion this cotransporter appears to be the major mechanism carrying chloride across the basolateral membrane. Consistent with this interpretation is the finding by Forbush and coworkers that the binding of benzmetanide, a potent inhibitor of the cotransporter, by shark rectal gland cell membranes is greatly increased by the activation of secretion and also by cell shrinkage [39, 40]. Haas, Johnson and Boucher also reported that the binding of bumetanide to cultured canine airway epithelia is greatly enhanced by activation of secretion and by cell shrinkage [41]. In airway epithelia the cotransporter may be up-regulated directly via a cAMP-dependent cascade and also as a secondary response to apical Cl channel activation [42]. It is also possible that the discrepancy between our results and those of Tanner, Maxwell and McAteer [12] could be due to a difference in the origin of the subcultures used in the two studies.

Effect of AVP

Grantham and coworkers have reported that AVP, an adenylate cyclase agonist, caused enlargement of MDCK cysts, caused fluid secretion by MDCK monolayers, and increased cellular levels of cAMP [8]. 1-Desamino-8-d-AVP, a V_2 receptor agonist, mimicked the effect of AVP. AVP had no effect on the hydraulic permeability of the MDCK epithelium and initiated secretion in the presence of identical solutions on both sides of the monolayer. We report here that the initiation of secretion is accompanied by a rapid and sustained loss of cell volume and by variable changes in membrane electrical potentials (Table 2). Hebert et al have reported that AVP increases both potassium and chloride conductances in the cell membranes of the mouse thick ascending limb [36, 38]. Moran and Valentich reported that forskolin has similar effects in the shark rectal gland [43]. We consider that the effects of AVP on membrane potential in the MDCK cyst are the consequence of two opposing effects of the secretagogue, an increase in potassium conductance in the basolateral membrane which would hyperpolarize the cell and activation of a chloride conductance in the apical membrane which, in the presence of an outwardly directed electrochemical gradient, permits the efflux of chloride, a current that tends to depolarize the cell. Variable degrees of activation of these two conductances, coupled with variable control membrane potentials and intracellular concentrations of chloride and potassium among the population of cysts examined may account for the variations in that data. We found that both control and experimental fluid transport rates were higher in cysts in which AVP caused depolarization than in cysts in which AVP caused hyperpolarization, suggesting that the control state of the cyst was a major factor. The loss of cell volume induced by AVP indicated the net loss of cation and anion from the cell. Inhibition of secretion by bumetanide in the presence of AVP hyperpolarized the cyst beyond the level existing in the control period but the drug had no effect in the absence of AVP. This supports both the activation of a depolarizing current by AVP (inhibitable by bumetanide) and the activation of a hyperpolarizing conductance (uncovered by the effect of bumetanide).

In conclusion, these results demonstrate the experimental advantages offered by the cultured cystic epithelium. The data obtained in preliminary experiments indicate that this methodology can be applied to the study of epithelial cells from human kidneys. The results are also consistent with the proposal that AVP induces fluid secretion by MDCK cells by activating an apical membrane chloride conductance, increasing basolateral membrane potassium conductance and activating a Na-Cl or a Na-K-2Cl cotransporter in the basolateral membrane. These results reinforce the conclusion that absorbing renal epithelial cells, albeit cultured cells, can be induced to reverse the direction of fluid transport [2].

Acknowledgments

A preliminary report of this work was published in abstract form (*J Am Soc Nephrol* 3:820, 1992). This work was supported by grant DK-45614 from NIH to J. Grantham and a grant-in-aid from the American Heart Association and a grant from the Polycystic Kidney Research Foundation to L. Sullivan. We thank Su Hao and Arlana Phillips for their technical assistance.

Reprint requests to Dr. L.P. Sullivan, Department of Physiology, University of Kansas Medical Center, 3901 Rainbow Blvd., Kansas City, Kansas 66160-7401, USA.

References

1. GRANTHAM JJ, WELLING LW, EDWARDS RM: Evaluation of function in single segments of isolated renal blood vessels, nephrons and collecting ducts, in *Handbook of Physiology. Section 8: Renal Physiology,* edited by WINDHAGER EE, New York, Oxford University Press, pp 351–384, 1992
2. GRANTHAM JJ: Fluid secretion, cellular proliferation and the pathogenesis of renal epithelial cysts. *J Am Soc Nephrol* 3:1843–1857, 1993
3. YE M, GRANTHAM JJ: The secretion of fluid by renal cysts from patients with autosomal dominant polycystic kidney disease. *N Engl J Med* 329:310–313, 1993
4. SIMMONS NL: Renal epithelial Cl^- secretion. *Exp Physiol* 78:117–137, 1993
5. MCATEER JA, EVAN AP, GARDNER EL: Morphogenetic clonal growth of kidney epithelial cell line MDCK. *Anat Rec* 217:229–239, 1987
6. GRANTHAM JJ, UCHIC M, CRAGOE EJ JR, KORNHAUS J, GRANTHAM JA, DONOSO V, MANGOO-KARIM R, EVAN A, MCATEER J: Chemical modification of cell proliferation and fluid secretion in renal cysts. *Kidney Int* 35:1379–1389, 1989
7. MANGOO-KARIM R, UCHIC M, LECHENE C, GRANTHAM JJ: Renal epithelial cyst formation and enlargement in vitro: Dependence on cAMP. *Proc Natl Acad Sci USA* 86:6007–6011, 1989
8. MANGOO-KARIM R, UCHIC ME, GRANT M, SHUMATE WA, CALVET JP, PARK CH, GRANTHAM JJ: Renal epithelial fluid secretion and cyst growth: The role of cyclic AMP. *FASEB J* 3:2629–2632, 1989
9. GRANT ME, NEUFELD TK, CRAGOE EJ JR, WELLING LW, GRANTHAM JJ: Arginine vasopressin stimulates net fluid secretion in a polarized subculture of cyst-forming MDCK cells. *J Am Soc Nephrol* 2:219–227, 1991

10. BROWN CDA, SIMMONS NL: Catecholamine-stimulation of Cl-secretion in MDCK cell epithelium. *Biochim Biophys Acta* 649:427–435, 1981
11. SIMMONS NL: Chloride secretion stimulated by prostaglandin E1 and by forskolin in a canine renal epithelial cell line. *J Physiol (Lond)* 432:459–472, 1991
12. TANNER GA, MAXWELL MR, MCATEER JA: Fluid transport in a cultured cell model of kidney epithelial cyst enlargement. *J Am Soc Nephrol* 2:1208–1218, 1991
13. MACIAS WL, MCATEER JA, TANNER GA, FRITZ AL, ARMSTRONG WM: NaCl transport by Madin Darby canine kidney cyst epithelial cells. *Kidney Int* 42:308–319, 1992
14. MANGOO-KARIM R, GRANTHAM JJ: Transepithelial water permeability in an in vitro model of renal cysts. *J Am Soc Nephrol* 1:278–286, 1990
15. WANG AZ, OJAKIAN GK, NELSON WJ: Steps in the morphogenesis of a polarized epithelium. II. Disassembly and assembly of plasma membrane domains during reversal of epithelial cell polarity in multicellular epithelial (MDCK) cysts. *J Cell Sci* 95:153–165, 1990
16. RINK TJ, MONTECUCCO C, HESKETH TR, TSIEN RY: Lymphocyte membrane potential assessed with fluorescent probes. *Biochim Biophys Acta* 595:15–30, 1980
17. WILSON HA, CHUSED TM: Lymphocyte membrane potential and Ca^{2+}-sensitive potassium channels described by oxonol dye fluorescence measurements. *J Cell Physiol* 125:72–81, 1985
18. BREUER WV, MACK E, ROTHSTEIN A: Activation of K and Cl channels by Ca and cyclic AMP in dissociated kidney epithelial cells. *Pflügers Arch* 411:450–455, 1988
19. SULLIVAN LP, WALLACE DP, CLANCY RL, GRANTHAM JJ: Effect of cellular acidosis on cell volume in S2 segments of renal proximal tubules. *Am J Physiol* 258:F831–F839, 1990
20. SULLIVAN LP, GRANTHAM JA, ROME L, WALLACE D, GRANTHAM JJ: Fluorescein transport in isolated proximal tubules in vitro: Epifluorometric analysis. *Am J Physiol* 258:F46–F51, 1990
21. WANG AZ, OJAKIAN GK, NELSON WJ: Steps in the morphogenesis of a polarized epithelium. I. Uncoupling the roles of cell-cell and cell-substratum contact in establishing plasma membrane polarity in multicellular epithelial (MDCK) cysts. *J Cell Sci* 95:137–151, 1990
22. MANGOO-KARIM R, GRANTHAM JJ: Transepithelial water permeability in an in vitro model of renal cysts (MDCK). *J Am Soc Nephrol* 1:278–285, 1990
23. ROTHSTEIN A, MACK E: Volume-activated K^+ and Cl^- pathways of dissociated epithelial cells (MDCK): Role of Ca^{2+}. *Am J Physiol* 258:C827–C834, 1990
24. KREMER SG, ZENG W, SKORECKI KL: Simultaneous fluorescence measurement of calcium and membrane potential responses to endothelin. *Am J Physiol* 263:C1302–C1309, 1992
25. MACIAS WL, MCATEER JA, TANNER GA, ARMSTRONG WM: Electrogenic chloride secretion by Madin-Darby canine kidney (MDCK)—cyst epithelial cells. (abstract) *J Am Soc Nephrol* 3:298, 1992
26. MCCANN JD, WELSH MJ: Regulation of Cl^- and K^+ channels in airway epithelium. *Annu Rev Physiol* 52:115–135, 1990
27. PETERSEN OH: Calcium-activated potassium channels and fluid secretion by exocrine glands. *Am J Physiol* 251:G1–G13, 1986
28. EPSTEIN FH, SILVA P: Na-K-Cl Cotransport in chloride-transporting epithelia. *Annals NY Acad Sci* 456:187–197, 1985
29. GREGER R, SCHLATTER E, WANG F, FORREST J: Mechanism of NaCl secretion in rectal gland tubules of spiny dogfish (Squalus Acanthias) 3. Effects of stimulation of secretion by cyclic AMP. *Pflügers Arch* 402:376–384, 1984
30. SMITH PL, WELSH MJ, STOFF JS, FRIZZELL RA: Chloride secretion be canine tracheal epithelium: I. Role of intracellular cAMP levels. *J Memb Biol* 70:217–226, 1982
31. KOLB HA, BROWN CDA, MURER H: Identification of a voltage-dependent anion channel in the apical membrane of a Cl-secretory epithelium (MDCK). *Pflügers Arch* 403:262–265, 1985
32. WEISS H, LANG F: Ion channels activated by swelling of Madin Darby canine kidney (MDCK) cells. *J Membrane Biol* 126:109–114, 1992
33. BANDERALI U, ROY G: Activation of K^+ and Cl^- channels in MDCK cells during volume regulation in hypotonic media. *J Membr Biol* 126:219–234, 1992
34. WELSH MJ: Barium inhibition of basolateral membrane potassium conductance in tracheal epithelium. *Am J Physiol* 244:F639–F645, 1983
35. GREGER RE, SCHLATTER F: Mechanism of NaCl Secretion in rectal gland tubules of spiny dogfish (Squalus-Acanthias) 2. Effect of Inhibitors. *Pflügers Arch* 402:364–375, 1984
36. HEBERT SC, ANDREOLI TE: Effects of antidiuretic hormone on cellular conductive pathways in mouse medullary thick ascending limbs of Henle: II. Determinants of the ADH-mediated increase in transepithelial voltage and in net Cl absorption. *J Membr Biol* 80:221–234, 1984
37. BEYENBACH KW, FROMTER E: Electrophysiological evidence for Cl secretion in shark renal proximal tubules. *Am J Physiol* 248: F282–F295, 1985
38. HEBERT SC, FRIEDMAN PA, ANDREOLI TE: Effects of antidiuretic hormone on cellular conductive pathways in mouse medullary thick ascending limbs of Henle: I. ADH increases transcellular conductance pathways. *J Membr Biol* 80:201–220, 1984
39. FORBUSH B, III, HAAS M, LYTLE C: Na-K-Cl cotransport in the shark rectal gland I. Regulation in the intact perfused gland. *Am J Physiol* 262:C1000–C1008, 1992
40. LYTLE C, FORBUSH B, III: Na-K-Cl cotransport in the shark rectal gland II. Regulation in isolated tubules. *Am J Physiol* 262:C1009–C1017, 1992
41. HAAS M, JOHNSON LG, BOUCHER RC: Regulation of Na-K-Cl cotransport in cultured canine airway epithelia: A [^{3}H]bumetanide binding study. *Am J Physiol* 259:C557–569, 1990
42. HAAS M, MCBRAYER DG, YANKASKAS JR: Dual mechanisms for Na-K-Cl cotransport regulation in airway epithelial cells. *Am J Physiol* 264:C189–C200, 1993
43. MORAN WM, VALENTICH JD: Cl^- secretion by cultured shark rectal gland cells. II. Effects of forskolin on cellular electrophysiology. *Am J Physiol* 260:C824–C831, 1991